Neurobiology of Disease 32 (2008) 1–9

Contents lists available at ScienceDirect

Neurobiology of Disease

journal homepage: www.elsevier.com/locate/ynbdi

Review

Rodent genetic models of Huntington disease

Mary Y. Heng [a,b], Peter J. Detloff [c], Roger L. Albin [a,b,d,*]

[a] Neuroscience Graduate Program, University of Michigan, Ann Arbor, MI, 48109, USA
[b] Department of Neurology, University of Michigan, Ann Arbor, MI, 48109, USA
[c] Department of Biochemistry and Molecular Genetics, University of Alabama at Birmingham, Birmingham, AL, 36294, USA
[d] Geriatrics Research, Education, and Clinical Center, VAAAHS, Ann Arbor, MI, 48105, USA

ARTICLE INFO

Article history:
Received 9 April 2008
Revised 13 June 2008
Accepted 15 June 2008
Available online 26 June 2008

Keywords:
Polyglutamine
Mouse
Striatum

ABSTRACT

Huntington disease (HD) is a dominantly inherited human neurodegenerative disorder characterized by motor deficits, cognitive impairment, and psychiatric symptoms leading to inexorable decline and death. Since the identification of the *huntingtin* gene and the characteristic expanded CAG repeat/polyglutamine mutation, multiple murine genetic models and one rat genetic model have been generated. These models fall into two general categories: transgenic models with ectopic expression of the characteristic expanded CAG codon mutation, and knock-in models with expression of mutant *huntingtin* under control of endogenous regulatory elements. Rodent genetic models are valuable tools for studying mechanisms of pathogenesis in HD and for preclinical evaluation of possible therapies. In this mini-review, we provide a concise comparative summary of rodent genetic models of HD.

Contents

Introduction

Huntington disease (HD) is an adult-onset, dominantly inherited human neurodegenerative disorder characterized by progressive motor impairment, involuntary movements, cognitive decline, and psychiatric disturbances. HD is caused by pathologic expansion of polymorphic CAG repeats in exon 1 of the *huntingtin* gene, translated as an expanded polyglutamine domain. *Huntingtin* encodes a widely expressed protein (huntingtin [htt]; Huntington's Disease Collaborative Research Group, (1993) and htt is a large, approximately 350 kD protein of elusive function. There is emerging evidence supporting important roles for htt in regulating transcription of brain-derived neurotrophic factor (BDNF), endocytic trafficking of neurotrophins with htt and htt associated proteins forming effector complexes that regulate endosome motility, and interaction with scaffolding proteins (Pal et al., 2008; Sun et al., 2001; Zuccato et al., 2003). Htt has a predominantly cytoplasmic localization and is expressed in virtually

* Corresponding author. 5023 BSRB, 109 Zina Pitcher Place, Ann Arbor, MI, 48109-2200, USA. Fax: +1 734 763 7686.
E-mail address: ralbin@umich.edu (R.L. Albin).
Available online on ScienceDirect (www.sciencedirect.com).

0969-9961/$ – see front matter © 2008 Elsevier Inc. All rights reserved.
doi:10.1016/j.nbd.2008.06.005

all neurons and some extra-neuronal tissues (Landwehrmeyer et al., 1995; Sharp et al., 1995; Strong et al., 1993). Disease-causing polyglutamine repeat mutations occur in eight other neurodegenerative disorders that exhibit regionally distinctive patterns of neurodegeneration (Orr and Zoghbi, 2007). Since the discovery of *huntingtin* and the characteristic mutation in 1993, a variety of rodent genetic models have been generated (Table 1). Rodent genetic models are potentially valuable as tools for exploring the pathogenesis of HD, in enabling the search for potential therapeutic targets, and in preclinical evaluation of potential therapies. Selection of experimental models depends on the validity of models, characteristics of models, and the type of experiments planned. In this review, we provide a comparative summary of the most widely used murine genetic models of HD, and the newer rat genetic model. The available rodent models can be separated into two categories: transgenic models (ectopic expression of the *huntingtin* mutation) and knock-in models (expression of the mutant *huntingtin* gene under the control of endogenous regulatory elements). These models vary repeat length, level of expression of mutant htt protein, and whether the mutant allele is truncated or full length, human or murine (Table 1).

HD clinical features and pathology

The clinical features and pathology of HD provide the standards for assessing validity of murine genetic models. In humans, median age of onset of HD occurs around 40 years with premature death approximately 15–20 years after onset of symptoms (Warby et al., 2008). Prevalence in populations of European ancestry is approximately 4–8 people per 100,000 (Harper, 1992) with a significantly larger number of individuals at risk for HD (Conneally, 1984). HD is much less common in populations of non-European ancestry. Normal *huntingtin* alleles contain less than 27 CAG repeats with a median around 18 (Kremer et al., 1994; Warby et al., 2008). Repeat numbers exceeding 39 result in full penetrance, and alleles with 36–39 CAG repeats are associated with reduced penetrance (Rubinsztein et al., 1996). Intergenerational transmission of mutant alleles often results in repeat number expansion and individuals with alleles carrying 27–35 CAG repeats will not develop HD but have increased risk of HD in their children (Semaka et al., 2006). There is a strong inverse correlation between CAG repeat length and age of onset of HD. CAG repeat length accounts for 42–73% of the variance in age of onset with 60 or more CAG repeats resulting in disease onset at 20 years of age or younger (Andresen et al., 2007; Andrew et al., 1993; Huntington's Disease Collaborative Research Group, 1993; Gusella and MacDonald, 1995; Langbehn et al., 2004; Stine et al., 1993). Manifest HD is defined clinically by the presence of a movement disorder, usually chorea but sometimes dystonia or bradykinesia. Data from the PREDICT-HD study of presymptomatic mutant allele carriers confirms clinical impressions and data from prior studies suggesting that onset of manifest HD is preceded by behavioral and cognitive changes (Duff et al., 2007; Johnson et al., 2007; Solomon et al., 2007). It is likely that behavioral and cognitive changes are followed by and or accompanied by relatively subtle declines in coordination. Incoordination progressively worsens and motor deficits eventually include dysarthria, dysphagia, and immobility (Penney et al., 1990). End-stage HD patients are profoundly debilitated and demented.

Neurodegeneration within the central nervous system exhibits a regionally selective pattern in HD, with medium spiny neurons (MSNs) of the striatum exhibiting the earliest degeneration and atrophy (Vonsattel et al., 1985). Cortical degeneration occurs also in early phases of HD (Rosas et al., 2002; 2005; 2008). Striatal and cortical degeneration and atrophy are ultimately profound (Halliday et al., 1998). Careful neuropathologic evaluations of more advanced HD specimens reveal evidence of neurodegeneration in many brain regions. Expression of *huntingtin* is widespread and probably universal among neurons, and there is no clear correlation between *huntingtin* expression and the regional pattern of initial pathology in HD (Landwehrmeyer et al., 1995; Sharp et al., 1995; Strong et al., 1993). As with other polyglutamine diseases, HD is marked by expression of neuronal intranuclear inclusions (NIIs) and cytoplasmic inclusions containing aggregated expanded repeat htt and other proteins (Becher et al., 1998; DiFiglia et al., 1997; Maat-Schieman et al., 1999).

Neuropathologic analysis is necessarily post-mortem analysis, but there is strong *in vivo* evidence of the inferred early changes in striatum and cortex. Imaging studies of pre-manifest and early manifest HD reveal substantial striatal and cortical atrophy (Aylward et al., 2000; 2004a; Beglinger et al., 2005; Rosas et al., 2005; Rosas et al., 2008), as well as decreases in striatally enriched dopamine D1 and D2 receptors (Antonini et al., 1996; Weeks et al., 1996). In pre-manifest HD mutant allele carriers, striatal atrophy may occur years prior to predicted age of onset of manifest HD (Aylward et al., 2000; 2004b).

Murine models of HD

A valid murine model of HD should recapitulate key features of HD. These should include mid- to late-life onset, progressive motor impairment, preferential early loss of striatal projection neurons, and expression of NIIs and cytoplasmic aggregates in an appropriate distribution. A valid model should exhibit measurable progressive pathology. Other possible criteria can be entertained but may not apply to rodents. Chorea, for example, is probably a phenomenon restricted to primates. HD is characterized by early cognitive and psychiatric abnormalities but determining their precise rodent analogues is problematic. Following are summaries of the behavioral phenotypes and pathologic features of selected murine genetic models of HD and the rat genetic model (Table 1; Fig. 1).

Transgenic rodent models

R6/2

Of the transgenic chimeric models that express truncated forms of the human mutant HD allele, the R6/2 line is the most widely used. This line expresses an exon 1 fragment of htt with a range of 148–153 repeats, expressed from an unknown location in the mouse genome. The R6/2 line displays an aggressive phenotype and provides clear experimental endpoints. R6/2 mice exhibit behavioral deficits by 5 weeks, neuroanatomic abnormalities including progressive reduction in brain and striatal volume, substantially reduced striatal neuron number by 12 weeks, and death by 12–15 weeks (Hickey et al., 2005; Mangiarini et al., 1996; Morton et al., 2005; Stack et al., 2005). Mice normally reach sexual maturity by 6 weeks and live beyond 2 years of age. Evaluation with learning and memory tasks shows abnormalities as early as 3.5 weeks of age, and simple motor tasks such as the rotorod and beam walking reveal deficits by 5 weeks of age (Carter et al., 1999; Lione et al., 1999; Stack et al., 2005). NIIs are present as early as post-natal day 1 in R6/2 striatum, somatosensory cortex, and hippocampal formation. These NIIs increase steadily in number, size, and distribution (Morton et al., 2000; Stack et al., 2005). Within the striatum, NIIs appear first in the matrix compartment (Morton et al., 2000). At disease endstage, R6/2 brain reveals widespread neuronal nuclear inclusions (NIIs) and neuropil aggregates (Morton et al., 2000; Stack et al., 2005). Total brain weight is decreased by 30 days (Stack et al., 2005). By 12 weeks, there is 26% reduction in striatal neuron number and a 41% reduction in striatal volume; however, total brain volume is reduced by 44% (Stack et al., 2005). The reduction in total brain volume is too large to be accounted for by the reduction in striatal volume alone, supporting the inference that there is diffuse loss of neurons in R6/2 brain. Striatal dopamine D1 and D2 receptors, highly enriched on dendrites of striatal projection neuron, are decreased as early as 8 weeks, consistent with both early striatal neuronal dysfunction and neurodegeneration (Cha et al., 1998a). Other neurotransmitter receptors are decreased at 12 weeks and some

Table 1
Rodent genetic models of HD

Line	CAG expansion and genetic expression	Age of onset and behavioral phenotype	Neuropathology	Survival	Additional phenotypes	References
N171-82Q (chimeric fragment transgenic) C57BL/6JxC3H/HeJ	N-terminal fragment expressing first 171 amino acids of human huntingtin; 82 repeats. Mouse PrP promoter.	Progressive weight loss beginning 4–6 weeks before death as well as tremor and hypokinesis, and clasping. Progressive accelerated rotarod deficit beginning at 12 weeks.	NIIs >50% observed in the cortex, hippocampus, amygdala, but less in the striatum. Astrocytic reactive gliosis and neuropil aggregates (GFAP, EM48–16 weeks). Neuronal loss and neurodegeneration in the cortex and sriatum, 20 weeks (TUNEL, cresyl violet staining, and EM).	20–24 weeks.	20–24 weeks.	Schilling et al. (1999) Yu et al. (2003)
R6/2 (chimeric fragment transgenic) CBAxC57BL/6 mix background strain	Human exon 1 N-terminal fragment: ~150 CAGs. HD promoter.	Progressive weight loss by ~8 weeks. Accelerated rotarod deficit visible at 5 weeks. Clasping, 6 weeks. Increase in limb movement, 10 weeks (video capture). Decrease in grip strength, 11 weeks (grip strength meter). Circling behavior, 12 weeks. Cognitive deficits: water Morris maze (3.5 weeks), T-maze (5 weeks), two choice swim tank (6.5 weeks), visual discriminate learning (7–8 weeks).	Onset of decreased brain weight, 4 weeks. 44% decrease in brain volume, 41% decrease in striatal volume, ~6-fold increase in ventricular volume, 12 weeks. Htt positive aggregates present by postnatal day 1 in cortical layers II, V, VI, neostriatum and greatest in the hippocampus. 25% reduction in striatal neuron number, 60% decrease in striatal neuron area and increase in reactive astrogliosis, 12 weeks. Widespread NIIs and neuropil aggregates, 12 weeks. Decrease in dopamine D1 and D2 receptors in striatum. Decrease in mGluR II, AMPA and kainate receptors in striatum and cortex, 12 weeks. Decrease in A2a adenosine receptors, 4 weeks.	12–15 weeks.	Seizures, diabetes, NMJ and cardiac dysfunction.	Carter et al. (1999) Cha et al. (1998a, b) Davies et al. (1997) Hickey et al. (2005) Hurlbert et al. (1999) Lione et al. (1999) Mangiarini et al. (1996) Meade et al. (2002) Mihm et al. (2007) Ribchester et al. (2004) Stack et al. (2005)
Full length *HD* Cdna (chimeric full length transgenic) FVB/N background strain	CMV promoter: 89 CAGs.	Clasping, 8 weeks. Hyperactive, unilateral rotation, excessive grooming, 20 weeks. Decrease in exploratory and locomotor activity, 24 weeks (by general monitoring).	PolyQ aggregates, 12 weeks. NIIs in cerebellum, cortex, hippocampus, thalamus, and <1% in striatum. Astrocytic reactive gliosis (GFAP). ~20% fewer striatal MSNs in homozygous (H and E and TUNEL staining).	Normal lifespan	Urinary incontinence	Reddy et al. (1998)
YAC 128 (chimeric full length transgenic) FVB/N background strain	Full length *HD*/mouse exon 1: 120 CAGs HD promoter.	Hyperkinetic, 12 weeks and hypokinetic, 48 weeks (open field). Accelerated rotarod deficit, 24 weeks. Progressive cognitive deficits, 8 weeks (accelerated rotarod), 32 weeks (water Morris maze, open field habituation, and T-maze).	10.4%–15% reduction in striatal and 7%–8.6%, reduction in cortical volumes, 48 weeks. 9.1% reduction in striatal neuron number and 8.3% reduction cortical neuron number, 48 weeks (stereology). Diffuse striatal htt nuclear immunoreactivity (EM48), 12 weeks >cortex, hippocampus, and cerebellum progressed and became more widespread but no NIIs detected, 48 weeks. EM 48 positive inclusions detected in striatal cells, 72 weeks. Increase in NMDA receptor binding (dentate gyrus, inner cortex, and whole brain), increase in AMPA (cerebellum and whole brain), mGluR I (whole brain) and mGluR II receptor binding (dentate gyrus and whole brain). No change in striatal dopamine, GABA-A/B or adenosine receptor binding at 48 weeks.	Normal lifespan.	None reported.	Benn et al. (2007) Hodgson et al. (1999) Slow et al. (2003) Van Raamsdonk et al. (2005a, 2005b)
BACHD (chimeric full length transgenic) FVB/NJ mix background	Full length human huntingtin: 97 CAGs. HD promoter.	Weight gain of 20–30% compared to WT between 8 weeks and 24 weeks. Maintained weight gain between 24 weeks and 48 weeks. Subtle but significant motor impairment initially at 8 weeks (accelerated rotarod) and progressed by 24 weeks.	Brains exhibited gross atrophy (48 weeks). 20% decrease in whole brain weight (minus the cerebellum and olfactory bulb) compared to WT. 32% decrease in cortical and 28% decrease in striatal volume 48 weeks (stereology). Degenerating darkly stained neurons 14% in the lateral striata, 48 weeks (toluidine blue staining, EM) No significant striatal neuron loss, 48 weeks (NeuN staining, stereology). mhtt inclusions predominantly found in neuropil and few in cortex and striatum, 48 and 72 weeks (hematoxylin and EM48).	Normal lifespan.	None reported.	Gray M. (2008)

(continued on next page)

Table 1 (*continued*)

Line	CAG expansion and genetic expression	Age of onset and behavioral phenotype	Neuropathology	Survival	Additional phenotypes	References
Transgenic HD Rat (chimeric fragment transgenic) Sprague–Dawley	*huntingtin* cDNA frament expressing 22% of the rat HD gene: 51 CAGs Rat promoter.	Weight loss, 96 weeks. Reduced anxiety-like behavior, 8 weeks (elevated plus maze). Cognitive decline 40 weeks(radial arm maze) and progressive motor impairment (accelerated rotarod). Involuntary movements of the head defined by abrupt, rapid, brief, and unsustained irregular movements of the neck, 60 weeks (open field testing).	Neuropil aggregates and nuclear inclusions predominantly in the striatum, occasional in cortex 72 weeks (EM48). Decrease in striatal dopamine and tryptophan levels 72 weeks (HPLC) Enlarged lateral ventricles and focal lesions in the striatum, 32 weeks (MRI). Reduced local cerebral rates of glucose metabolism, 32 weeks (FDG-PET imaging). No significant cell loss reported.	98 weeks.	None reported.	von Horsten et al. (2003) Cao et al. (2006).
Hdh/Q72-80 (knock-in) 129/Svx C57BL/6 mix background strain or 129/Svx FVB/N mix background strain	*Hdh* promoter: 72–80 CAGs.	Increased male aggression and a lesser extent in females, 12 weeks. No observed weight loss compared to WT, 72 weeks. rotarod (nonaccelerated) deficit beginning at 16 weeks (C57BL/6 N6 generation)	H and E, Nissl stains, and GFAP immunoreactivity revealed no neuron loss or reactive gliosis. No NIIs detected. No loss in enkephalin or calbindin immunoreactivity, 72 weeks. Neuropil aggregates, 28–96 weeks. Striatal nuclear htt aggregates, 96 weeks (C57BL/6 N6-7 generation or FVB/N N4 generation). Decrease in dopamine D2 receptor binding and increase in GABA/benzodiazepine receptor binding in the striatum and cortex, 68–72 weeks.	Normal lifespan.	None reported.	Kennedy et al. (2005) Shelbourne et al. (1999)
HdhQ111 (knock-in) 129/CD1 mix background strain	Chimeric human/mouse exon1: 109 CAGs. Hdh promoter.	Gait impairment 96 weeks (painted-feet). No accelerated rotarod deficits.	Diffuse striatal nuclear-reactivity, 6 weeks (EM48). NIIs, 48 weeks. Striatal neuropil aggregates, 68 weeks. Neurodegeneration and reactive gliosis, 96 weeks (toluidine blue GFAP).	Normal lifespan	None reported.	Wheeler et al. (2000, 2002)
HdhQ140 (knock-in) 129Sv/C57BL6 mix background strain	Chimeric human/mouse exon1: 140 CAGs. Hdh promoter.	No obvious abnormal behavior up to 48 weeks. No abnormal weight loss. Decrease in locomotor activity, 8–24 weeks (open field). Hyperactivity, 4 weeks and hypoactivity, 12 weeks. Gait abnormalities, 48 weeks (painted-feet).	Striatal htt nuclear staining beginning at 8 weeks and becoming more widespread by 24 weeks. nuclear and neuropil aggregates prominent at 16 weeks in the striatum, nucleus accumbens, olfactory tubercle (EM48), as well as widespread nuclear staining including cortical layers II/III, and V., hippocampus, and regions of the olfactory system.	Normal lifespan.	None reported.	Menalled et al. (2003)
Hdh(CAG)150 (knock-in) 129/ Ola and C57BL/J6 mix background strain	Murine Hdh: 150 CAGs. Hdh promoter.	Motor abnormalities: Accelerated rotarod, Balance beam, painted-feet, 70–100 weeks. Resting tremor and ataxic, 100 weeks.	Striatal nuclear htt immunoreactivity, 28 weeks. Striatal NIIs, 37 weeks. Reactive astrocytic gliosis, 56 weeks. Robust striatal NIIs and striatal neuron receptor loss, 70–100 weeks. Loss of striatal perikarya and volume, 100 weeks. Decrease in striatal dopamine D1 and D2 receptors and dopamine transporters (DAT).	Normal lifespan.	None reported.	Heng et al. (2007) Lin et al. (2001) Tallaksen-Greene et al. (2005)

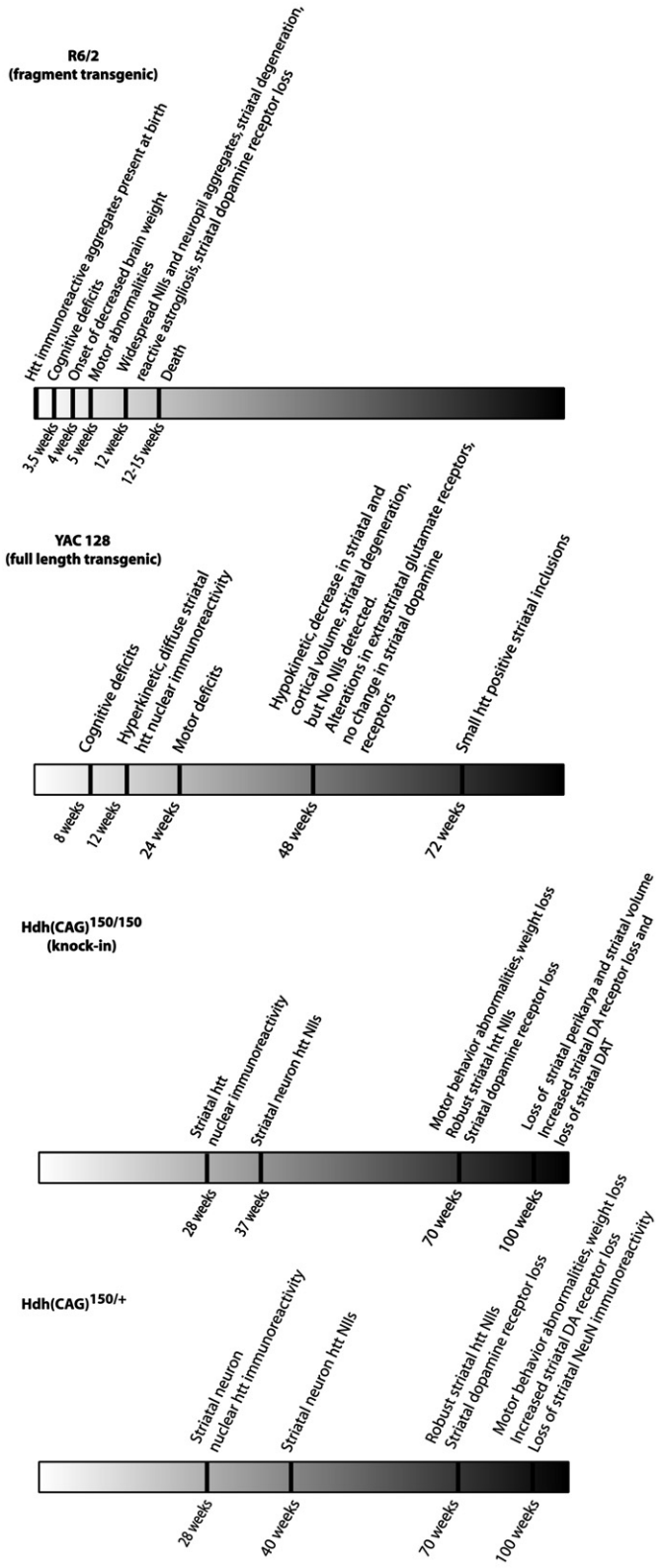

Fig. 1. Timelines of selected murine genetic models of HD.

receptor mRNA expression levels are decreased as early as 4 weeks (Cha et al., 1998b; 1999).

The aggressive phenotype makes R6/2 very useful for preclinical pharmacology, but it is not an exact genetic or neuropathological analogue of adult-onset HD. R6/2 mice have widespread NII expression, a high incidence of epilepsy, diabetes, cardiac dysfunction, and neuromuscular junction abnormalities, none of which are characteristic of typical adult-onset HD (Hurlbert et al., 1999; Meade et al., 2002; Mihm et al., 2007; Ribchester et al., 2004). As the R6/2 model exhibits severe, early onset and diffuse pathology, it is potentially a good model of juvenile-onset HD, where effects of expanded polyglutamine htt occur in the context of a developing brain. Epilepsy, for example, is common in juvenile-onset HD (Seneca et al., 2004).

YAC128

The YAC128 is a widely used yeast artificial chromosome full length human mutant HD transgenic model generated and characterized by the Hayden laboratory (Slow et al., 2003; Van Raamsdonk et al., 2005a). YAC128 mice exhibit motor abnormalities as early as 3 months with increased open field activity, followed by rotorod performance abnormalities at 6 months. Behavioral deficits are progressive and by 12 months, open field activity is diminished significantly in comparison with controls. Van Raamsdonk et al. (2005b) evaluated YAC128 mice with a variety of more cognitively oriented tests, demonstrating abnormalities which precede and then parallel the progression of simpler motor function tests. Modest striatal atrophy is found at 9 months with both striatal and cortical atrophy at 12 months (10–15% and 7–8% decreases in volume, respectively). Unlike R6/2 mice, where there is probably diffuse loss of brain, other brain regions such as the cerebellum and hippocampal formation exhibit normal volume (Van Raamsdonk et al., 2005b). A modest degree of striatal neuron loss, approximately 15%, is found at 12 months. Although NIIs are not found until 18 months, abnormally high nuclear htt immunoreactivity is present within striatal and other neurons from 2 months onwards. Nuclear htt immunoreactivity is abundant in striatal neurons at 3 months of age and found in a significant number of cortical, hippocampal, and cerebellar neurons at the same age. By 6 months, nuclear htt immunoreactivity is present in many neurons (Van Raamsdonk et al., 2005b). YAC128 mice have a surprising feature; twelve month old YAC128 mice, despite the presence of behavioral abnormalities and evidence of striatal neuron loss, exhibit no decreases in a wide array of striatal neurotransmitter receptor binding sites (Benn et al., 2007). YAC128 mice display modest glutamate receptor binding site increases in some extrastriatal regions. NMDA receptor binding is increased in the hippocampus and cortical layers, AMPA receptor binding is increased in the cerebellum, and group 2 metabotropic glutamate receptor binding is increased in the dentate gyrus of the hippocampus (Benn et al., 2007). The apparently normal striatal neurotransmitter receptor expression is different from results with other murine genetic models and probably also HD, where neurotransmitter receptor expression appears to be a reliable indicator of striatal neuron dysfunction/degeneration.

Transgenic HD-like rat

The transgenic rat model of HD expresses a truncated *huntingtin* cDNA fragment expressing 22% of the rat HD gene. This fragment encodes 51 CAG repeats driven by the endogenous *huntingtin* rat promoter producing a truncated human/rat chimeric protein (von Horsten et al., 2003). The transgenic rat model exhibits a late onset neurological phenotype and develops gradually progressive motor abnormalities. They have reduced body weight gain followed by weight loss compared to wild type controls and are 20% lighter than controls at 24 months. Rapid weight loss at 24 months is often followed by death. Tremor, ataxia, clasping, limb dyskinesias, and seizures are not described. Involuntary head and neck movements are reported at 20 months of age when rats are observed in an open field setting (Cao et al., 2006). Transgenic HD-like rats exhibit reduced anxiety-like behaviors in the elevated plus maze test at 2 months and exhibit cognitive decline in spatial learning at 10 months. Accelerated rotarod dysfunction is observed as early as 10 months and progressively worsens by 15 months. Neuropathological examination reveals

neuropil aggregates and nuclear inclusions, predominantly expressed in the striatum, with occasional aggregates observed in the cortex at 18 months. High performance liquid chromatography analyses exhibit 80% striatal dopamine reduction in homozygotes while heterozygotes exhibit 20% striatal dopamine reduction compared to non-transgenic controls. Magnetic resonance imaging reveals enlarged lateral ventricles and focal lesions in the striatum at 8 months. [^{18}F]Fluoro-deoxyglucose positron emission tomography reveals reductions in striatal glucose metabolism at 8 months. No neuronal loss is described but stereological assessment of regional neuronal numbers and volumes is not reported.

The transgenic rat HD model is advantageous because of its larger brain mass. The transgenic rat model facilitates detailed neuroanatomic characterization and examination with non-invasive imaging methods, particularly PET imaging. Interventions using surgical approaches, such as neurotransplantation, are much easier in the larger rat brain.

Knock-in murine models

In contrast to the transgenic murine models of HD, knock-in models express mutant htt in an appropriate genomic and protein context. A number of knock-in models have been generated (Menalled, 2005). Experience with these models was initially disappointing, as they did not develop the marked phenotype of transgenic fragment models like R6/2. Careful analyses and generation of knock-in models with longer repeat lengths demonstrated behavioral and histological abnormalities in several knock-in models. In general, these models tend to show normal life span, milder initial behavioral abnormalities, development of more robust behavioral abnormalities at later ages, and expression of aggregate pathology more selectively localized to striatal neurons (Menalled, 2005; Table 1). There are several prospectively characterized knock-in models with larger CAG expansions and overt behavioral and neuropathological abnormalities (Menalled, 2005; Table 1; Fig. 1).

HdhQ94 and Hdh Q140

The HdhQ94 and HdhQ140 lines are based on a gene targeted replacement of exon 1 of the mouse *huntingtin* homologue, *Hdh*, with a chimeric mouse/human exon 1 coding for approximately 94 or 140 CAG repeats. In HdhQ94 mice, increased repetitive rearing is found at 2 months of age with decreased locomotion at 4 and 6 months of age (Menalled et al., 2002). Diminished striatal enkephalin mRNA expression is found at 4 months of age. In 18 to 26 month old mice, striatal volume is decreased by approximately 15% but striatal neuron number is normal. Nuclear htt immunoreactive microaggregates, which may be small NIIs, are observed in many striatal neurons by 6 months of age; these are found in striosome compartment neurons. Only rare nuclear microaggrates are described in cortex at 6 months and none in the hippocampal formation. Typical large striatal NIIs do not appear until 18 months of age and there is no mention of NIIs or cytoplasmic aggregates in other regions.

HdhQ140 mice exhibit similar but more pronounced features (Menalled et al., 2003). Increased repetitive rearing occurs at 1 month of age with diminished locomotor activity at 4 months of age. Footprint analysis at age 12 months reveals significant changes in mutant mouse gait. Striatal htt nuclear immunoreactivity is observed at 2 months with some nuclear microaggregates expressed. By 4 months, nuclear htt immunoreactivity becomes more intense and nuclear microaggreates are common. Other brain regions, including olfactory bulb, anterior olfactory nucleus, and piriform cortex, exhibit strong nuclear htt immunoreactivity. By 6 months, nuclear htt immunoreactivity and some microaggregates/NIIs are present in several brain regions; striatal nuclear htt immunoreactivity is more intense and large NIIs are expressed. Neuropil htt immunoreactive aggregates, presumably cytoplasmic inclusions, appear in striatum and other regions by 4 months and increase in density by 6 months of age. Neuropil aggregates are particularly prominent in the hippocampal formation, some cortical laminae, the globus pallidus, entopeduncular nucleus, and substantia nigra pars reticulata. In the latter three regions, they may be expressed in striatal neuron terminals. Striatal neuron loss and atrophy has not been demonstrated.

HdhQ111

Like the HdhQ94 and HdhQ140 lines, HdhQ111 is a knock-in model based on a chimeric human/mouse exon 1 construct (Wheeler et al., 2000; 2002). In this line, subtle motor deficits are detected by footprint analysis at 24 months of age. At this age, small numbers of degenerating striatal neurons are observed with reactive gliosis (Wheeler et al., 2002). In HdhQ111 homozygotes, clusters of ventral striatal neurons exhibit nuclear htt immunoreactivity at 1.5 months of age. By 4.5 months of age, there is strong nuclear htt immunoreactivity in many MSNs with some small NIIs formed. In HdhQ111 heterozygotes, prominent nuclear htt immunoreactivity is observed at 5 months of age. In both homozygotes and heterozygotes, older mice display prominent NIIs, and neuropil htt immunoreactive aggregates are found in the globus pallidus and substantia nigra pars reticulata by 17 months of age.

Hdh$^{(CAG)150}$

The *Hdh*$^{(CAG)150}$ knock-in mouse lacks foreign DNA sequences or selectable markers and is purely murine with approximately 150 CAG repeats inserted into exon 1 of the murine *huntingtin* homologue (Heng et al., 2007; Lin et al., 2001; Tallaksen-Greene et al., 2005). *Hdh*$^{(CAG)150}$ mice exhibit an apparently normal phenotype until greater than a year of age. At 100 weeks of age, homozygous *Hdh*$^{(CAG)150}$ mice exhibit weight loss, diminished activity, and abnormal rotorod performance. Both 100 week old homozygous and heterozygous *Hdh*$^{(CAG)150}$ mice display abnormal performance on a balance beam task and with footprint analysis. Qualitative changes in gait are apparent on the beam task in some homozygous mutants as early as 50 weeks of age. Evaluation of younger *Hdh*$^{(CAG)150}$ mice, less than 1 year of age, with the Morris water maze, fear conditioning, and open field testing did not show any abnormalities (Heng et al., unpublished data). At 100 weeks of age, stereological analysis demonstrates approximately 50% loss of neurons in heterozygous and homozygous *Hdh*$^{(CAG)150}$ mice, though only the homozygous *Hdh*$^{(CAG)150}$ mice exhibit loss of striatal volume (Heng et al., 2007). The latter fact suggests neuronal dysfunction rather than death in *Hdh*$^{(CAG)150}$ heterozygotes. Ultrastuctural study of 14 month old *Hdh*$^{(CAG)150}$ heterozygotes demonstrated striatal axonal degeneration (Yu et al., 2003). Assessment of striatal D1 and D2 receptor binding sites in 100 week old heterozygous and homozygous *Hdh*$^{(CAG)150}$ mice shows significant declines in these binding sites, greater in homozygous than heterozygous mutants. At 70 weeks of age, stereologic analyses showed normal striatal volume and striatal neuron number in both homozygous and heterozygous *Hdh*$^{(CAG)150}$ mice. Striatal D1 and D2 receptor binding sites are, however, diminished in 70 week old heterozygous and to a greater extent, homozygous *Hdh*$^{(CAG)150}$ mice. Normal striatal neuron number and volume in 70 week old *Hdh*$^{(CAG)150}$ mice, coupled with the presence of striatal D1 and D2 receptor binding deficits and behavioral changes, supports the inference that a period of neuronal dysfunction precedes neurodegeneration. As with other knock-in models, nuclear localization of htt immunoreactivity precedes NII formation. Nuclear htt immunoreactivity is found at 27–29 weeks of age. At approximately 40 weeks of age, some striatal neurons express NIIs, and by 70 weeks of age, NIIs are expressed by most striatal neurons. NIIs initially appear in clusters of striatal neurons predominantly within the matrix compartment. Around 100 weeks of age, almost all striatal neurons express NIIs. Even at this advanced age, NIIs are found in only a small minority of neurons in most other brain regions. Only piriform cortex and layer 4 of primary somatosensory cortex exhibit high percentages of neurons with NIIs. Neuropil

aggregates are abundant in the globus pallidus and substantia nigra pars reticulata, suggesting localization within striatal neuron terminals. The relatively selective distribution of NIIs in *Hdh*$^{(CAG)150}$ mice suggests preferential striatal pathology. This inference is consistent with GABA-A/benzodiazepine receptor binding studies in 100 week old *Hdh*$^{(CAG)150}$ mice. Extrastriatal regions that express high levels of GABA-A/benzodiazepine receptor binding sites exhibit normal binding.

Validity

While no rodent genetic model replicates all features of HD, rodent models provide valuable tools to study HD. Extrapolating from rodent models to HD depends on the validity of the model. Rodent genetic HD models can be assessed with the three criteria proposed by Paul Willner (Willner, 1991) with the goal of increasing the odds that results in the model will predict similar results in humans. First is face validity: does the phenotype of the model recapitulate the clinical manifestations of the disease of interest? Second is construct validity: do the experimental manipulations produce similar underlying mechanisms of pathogenesis as observed in the disease of interest? This may be the most challenging to establish, and is the critical since a model can have face validity driven by an irrelevant molecular mechanism. Third is predictive validity: is the model able to predict pathological outcomes known to exacerbate or ameliorate physiological states in the disease of interest (such as the response to therapeutic drugs)? There are difficulties in creating a valid model of HD when the disease itself is not fully understood, however, these criteria provide a framework to evaluate a wide range of models and allow systematic assessment of murine genetic models (Table 2).

Face validity can be assessed by comparison with the clinical and pathologic features of HD. Transgenic fragment, transgenic full length, and knock-in models all possess at least some face validity in that they recapitulate some of the phenotypic features of HD. All result in progressive motor dysfunction, and where assessed, progressive pathologic changes. In terms of behavioral features, the mid- to late-life onset of transgenic full length and knock-in murine models and the rat transgenic model appear to replicate typical adult-onset HD best. In terms of pathology, transgenic full length and knock-in murine models appear to replicate best the features of adult-onset HD with more selective striatal involvement than the R6/2 line. As mentioned above, however, the R6/2 line may resemble the more aggressive juvenile-onset form of HD.

Transgenic fragment, transgenic full length, and knock-in models all possess considerable construct validity. All express the expanded polyglutamine repeat domain that is the core cause of neurodegeneration in HD and other polyglutamine diseases (Ordway et al., 1997). Recent results, however, indicate that the specific regional pathology of individual polyglutamine diseases is a function of the biology of the protein carrying the pathologically expanded polyglutamine repeat (Orr and Zoghbi, 2007). Transgenic fragment models may be more models of generalized expanded polyglutamine repeat pathogenesis than of any specific polyglutamine disease. The expedience of an aggressive phenotype therefore must be balanced against the possibility that the phenotype may be driven by molecular processes that do not mimic HD. For this reason, transgenic full length and knock-in models appear to possess a greater degree of construct validity. Theoretically, knock-in models possess a yet higher degree of construct validity than transgenic full length models because the expanded CAG repeat sequence is expressed in its native biologic context. Huntingtin and its murine homologue are very similar proteins and likely to have similar functional properties.

Predictive validity is the most pragmatically important of Willner's criteria. The R6/2 line has been the major vehicle for preclinical pharmacology for HD. A substantial number of interventions have been evaluated with this line. Assessment of predictive validity requires comparison of model and human trial outcomes. The human experience is limited to date. The first large efficacy trial for HD, Coenzyme Q10 and Remacemide Evaluation in HD (CARE-HD), evaluated 600 mg per day of coenzyme Q10 and 600 mg per day of remacemide, a non-selective NMDA receptor antagonist (Huntington Study Group, 2001). Neither compound was effective though there was a trend towards efficacy with coenzyme Q10. Both compounds were evaluated subsequently in R6/2 mice and both treatments produced modest but significant amelioration of the R6/2 phenotype (Ferrante et al., 2002). On a mg/kg basis, mice in this study received much higher doses of coenzyme Q10 and remacemide than participants in the CARE-HD trial. Comparison of mouse and human results is confounded by probable differences in pharmacokinetics and effective doses. Mice in the simple cage environment, for example, may tolerate relatively higher doses of a psychoactive compound like remacemide. A second major efficacy study of coenzyme Q10, Coenzyme Q10 in Huntington Disease (2CARE), is now underway. 2CARE uses a substantially higher dose of coenzyme Q10 and should provide a definitive answer about the neuroprotective value of coenzyme Q10 in HD. 2CARE and other human efficacy

Table 2
Validity of representative models

Similarity of model to HD	Phenotypic	Molecular mechanism	Therapeutic response
Willner criteria	Face validity	Construct validity	Predictive validity
R6/2	+ Progressive motor phenotype. NII and cytoplasmic aggregate pathology. Very early onset and widespread pathology. Extra-CNS features not typical of HD.	++ Core feature — polyQ expansion. Lacks appropriate surrounding protein context and regulatory elements. Transcriptome alterations similar to HD.	U Coenzyme Q10 and remacemide unsuccessful in HD, efficacious in R6/2. Higher dose Q10 trial in progress.
YAC128	++1/2 Progressive motor phenotype, adult-onset, early cognitive features. Preferential striatal and cortical atrophy. Early nuclear htt immunoreactivity with late NIIs. No HD-like striatal neurotransmitter receptor changes.	++1/2 Core feature — polyQ expansion. Appropriate surrounding protein context. Ectopic location, lacks native murine regulatory elements.	U
Hhd(CAG)150	+++ Progressive motor phenotype. Mid-life onset. Preferential striatal degeneration and NII expression. Striatal neurotransmitter receptor changes precede neurodegeneration.	+++ Core feature — polyQ expansion. Appropriate surrounding protein context. Native murine regulatory elements. Transcriptome alterations similar to HD.	U

+ = some validity; ++ = considerable validity; +++ = excellent validity; U = unknown validity.

trials may provide useful information about the predictive validity of the R6/2 model. The R6/2 model has the most preclinical data available and more studies involving preclinical evaluation of other models are needed to assess their predictive validity.

Comparing models

While predictive validity of HD rodent genetic models is unknown, transgenic full length and knock-in models appear to possess better face and construct validity than transgenic fragment models. Accumulating human data to assess predictive validity will take years. In the interim, useful data might be gleaned by selective evaluation of compounds that succeed in R6/2 by further testing in transgenic full length or knock-in models. The practical advantages of the strong R6/2 phenotype makes it unlikely that it will be replaced as the preferred model for preclinical pharmacology, however, transgenic full length and knock-in murine models are probably the preferred models for experiments examining the pathogenesis and pathophysiology of HD.

Among transgenic full length and knock-in murine models, the YAC128 and *Hdh*$^{(CAG)150}$ lines offer the advantages of well characterized natural history and well characterized behavioral and pathologic endpoints. The *Hdh*$^{(CAG)150}$ line probably exhibits a period of neuronal dysfunction prior to neurodegeneration that should be especially valuable for examining early events in HD pathogenesis. Kuhn and colleagues (Kuhn et al., 2007) compared striatal gene expression changes in several murine genetic models of HD, including R6/2, YAC128, and *Hdh*$^{(CAG)150}$ (termed CHL2 in Kuhn et al., 2007) with striatal gene expression changes in HD. All murine genetic models had significant correlation with human striatal gene expression changes. The highest correlations were found with 22 month old *Hdh*$^{(CAG)150}$ homozygotes and 12 week old R6/2 mice. The most marked similarities between HD and murine genetic models occurred with down regulated transcripts. Similar results were obtained with a limited number of transcripts by Woodman and colleagues (Woodman et al., 2007). This may reflect the fact that *Hdh*$^{(CAG)150}$ homozygote and R6/2 mice of these ages exhibit the greatest degree of striatal degeneration among murine genetic models of HD.

The transgenic rat model possesses advantages due to its larger brain size and has a well defined natural history. As a transgenic fragment line, it theoretically possesses a lesser degree of construct validity than murine full length transgenic or knock-in models but this may be mitigated slightly by use of rat promoter sequences. Detailed neuropathologic examination of this model would be worthwhile. Its advantages must be balanced against the increased expense of maintaining larger rodents for months.

Summary

A variety of rodent genetic models of HD are available. The different features of these models confer different advantages and disadvantages, depending on specific experimental aims. Prudence dictates that no specific line should be regarded as “the model” of HD. Interesting results obtained in one line should be evaluated in other lines. While none of the models fulfill all Willner criteria, murine transgenic full length and particularly knock-in models appear to be the most loyal model of HD with age-appropriate onset, and behavioral deficits and neuropathology similar to HD. The milder phenotype and late onset of behavioral abnormalities of transgenic full length and knock-in murine models make them difficult to use for preclinical pharmacology. Knock-in models exhibit a natural history of behavioral deficits and striatal dysfunction followed by degeneration, allowing examination of early events in the pathogenesis of HD. Transgenic fragment models like R6/2 provide robust endpoints for preclinical pharmacology, but may involve pathophysiologic processes not typical of HD. Additional comparative studies of various rodent genetic HD models and with human trial data are needed to evaluate model validity completely.

References

Andresen, J.M., et al., 2007. The relationship between CAG repeat length and age of onset differs for Huntington's disease patients with juvenile onset or adult onset. Ann. Hum. Genet. 71, 295–301.

Andrew, S.E., et al., 1993. The relationship between trinucleotide (CAG) repeat length and clinical features of Huntington's disease. Nat. Genet. 4, 398–403.

Antonini, A., et al., 1996. Striatal glucose metabolism and dopamine D2 receptor binding in asymptomatic gene carriers and patients with Huntington's disease. Brain 119 (Pt 6), 2085–2095.

Aylward, E.H., et al., 2000. Rate of caudate atrophy in presymptomatic and symptomatic stages of Huntington's disease. Mov. Disord. 15, 552–560.

Aylward, E.H., et al., 2004a. Onset and rate of striatal atrophy in preclinical Huntington disease. Neurology. 63, 66–72.

Aylward, E.H., et al., 2004b. Onset and rate of striatal atrophy in preclinical Huntington disease. Neurology. 63, 66–72.

Becher, M.W., et al., 1998. Intranuclear neuronal inclusions in Huntington's disease and dentatorubral and pallidoluysian atrophy: correlation between the density of inclusions and IT15 CAG triplet repeat length. Neurobiol. Dis. 4, 387–397.

Beglinger, L.J., et al., 2005. White matter volume and cognitive dysfunction in early Huntington's disease. Cogn. Behav. Neurol. 18, 102–107.

Benn, C.L., et al., 2007. Glutamate receptor abnormalities in the YAC128 transgenic mouse model of Huntington's disease. Neuroscience. 147, 354–372.

Cao, C., et al., 2006. Progressive deterioration of reaction time performance and choreiform symptoms in a new Huntington's disease transgenic ratmodel. Behav. Brain Res. 170, 257–261.

Carter, R.J., et al., 1999. Characterization of progressive motor deficits in mice transgenic for the human Huntington's disease mutation. J. Neurosci. 19, 3248–3257.

Cha, J.H., et al., 1998a. Altered neurotransmitter receptor expression in transgenic mouse models of Huntington's disease. Philos. Trans. R. Soc. Lond. B. Biol. Sci. 354, 981–989.

Cha, J.H., et al., 1998b. Altered brain neurotransmitter receptors in transgenic mice expressing a portion of an abnormal human huntington disease gene. Proc. Natl. Acad. Sci. U. S. A. 95, 6480–6485.

Cha, J.H., et al., 1999. Altered neurotransmitter receptor expression in transgenic mouse models of Huntington's disease. Philos. Trans. R. Soc. Lond. B. Biol. Sci. 354, 981–989.

Conneally, P.M., 1984. Huntington disease: genetics and epidemiology. Am. J. Hum. Genet. 36, 506–526.

Davies, S.W., Turmaine, M., Cozens, B.A., DiFiglia, M., Sharp, A.H., Ross, C.A., Scherzinger, E., Wanker, E.E., Mangiarini, L., Bates, G.P., 1997. Formation of neuronal intranuclear inclusions underlies the neurological dysfunction in mice transgenic for the HD mutation. Cell 90, 537–548.

DiFiglia, M., et al., 1997. Aggregation of huntingtin in neuronal intranuclear inclusions and dystrophic neurites in brain. Science 277, 1990–1993.

Duff, K., et al., 2007. Psychiatric symptoms in Huntington's disease before diagnosis: the predict-HD study. Biol. Psychiatry. 62, 1341–1346.

Ferrante, R.J., et al., 2002. Therapeutic effects of coenzyme Q10 and remacemide in transgenic mouse models of Huntington's disease. J. Neurosci. 22, 1592–1599.

Gray, M., et al., 2008. Full-length human mutant huntingtin with a stable polyglutamine repeat can elicit progressive and selective neuropathogenesis in BACHD mice. J. Neurosci. 28, 6182–6195.

Gusella, J.F., MacDonald, M.E., 1995. Huntington's disease: CAG genetics expands neurobiology. Curr. Opin. Neurobiol. 5, 656–662.

Halliday, G.M., et al., 1998. Regional specificity of brain atrophy in Huntington's disease. Exp. Neurol. 154, 663–672.

Harper, P.S., 1992. The epidemiology of Huntington's disease. Hum. Genet. 89, 365–376.

Heng, M.Y., et al., 2007. Longitudinal evaluation of the Hdh(CAG)150 knock-in murine model of Huntington's disease. J. Neurosci. 27, 8989–8998.

Hickey, M.A., et al., 2005. Early behavioral deficits in R6/2 mice suitable for use in preclinical drug testing. Neurobiol. Dis. 20, 1–11.

Hodgson, J.G., Agopyan, N., Gutekunst, C.A., Leavitt, B.R., LePiane, F., Singaraja, R., Smith, D.J., Bissada, N., McCutcheon, K., Nasir, J., Jamot, L., Li, X.J., Stevens, M.E., Rosemond, E., Roder, J.C., Phillips, A.G., Rubin, E.M., Hersch, S.M., Hayden, M.R., 1999. A YAC mouse model for Huntington's disease with full-length mutant huntingtin, cytoplasmic toxicity, and selective striatal neurodegeneration. Neuron 23, 181–192.

Huntington Collaborative Research Group, 1993. A novel gene containing a trinucleotide repeat that is expanded and unstable on Huntington's disease chromosomes. Cell 72, 971–983.

Huntington Study Group, 2001. A randomized, placebo-controlled trial of coenzyme Q10 and remacemide in Huntington's disease. Neurology 57, 397–404.

Hurlbert, M.S., et al., 1999. Mice transgenic for an expanded CAG repeat in the Huntington's disease gene develop diabetes. Diabetes. 48, 649–651.

Johnson, S.A., et al., 2007. Beyond disgust: impaired recognition of negative emotions prior to diagnosis in Huntington's disease. Brain 130, 1732–1744.

Kennedy, L., Shelbourne, P.F., Dewar, D., 2005. Alterations in dopamine benzodiazepine receptor binding precede overt neuronal pathology in mice modelling early Huntington disease pathogenesis. Brain Res. 1039, 14–21.

Kremer, B., et al., 1994. A worldwide study of the Huntington's disease mutation. The sensitivity and specificity of measuring CAG repeats. N. Engl. J. Med. 330, 1401–1406.

Kuhn, A., et al., 2007. Mutant huntingtin's effects on striatal gene expression in mice recapitulate changes observed in human Huntington's disease brain and do not

differ with mutant huntingtin length or wild-type huntingtin dosage. Hum. Mol. Genet. 16, 1845–1861.
Landwehrmeyer, G.B., et al., 1995. Huntington's disease gene: regional and cellular expression in brain of normal and affected individuals. Ann. Neurol. 37, 218–230.
Langbehn, D.R., et al., 2004. A new model for prediction of the age of onset and penetrance for Huntington's disease based on CAG length. Clin. Genet. 65, 267–277.
Lin, C.H., et al., 2001. Neurological abnormalities in a knock-in mouse model of Huntington's disease. Hum. Mol. Genet. 10, 137–144.
Lione, L.A., et al., 1999. Selective discrimination learning impairments in mice expressing the human Huntington's disease mutation. J. Neurosci. 19, 10428–10437.
Maat-Schieman, M.L., et al., 1999. Distribution of inclusions in neuronal nuclei and dystrophic neurites in Huntington disease brain. J. Neuropathol. Exp. Neurol. 58, 129–137.
Mangiarini, L., et al., 1996. Exon 1 of the HD gene with an expanded CAG repeat is sufficient to cause a progressive neurological phenotype in transgenic mice. Cell 87, 493–506.
Meade, C.A., et al., 2002. Cellular localization and development of neuronal intranuclear inclusions in striatal and cortical neurons in R6/2 transgenic mice. J. Comp. Neurol. 449, 241–269.
Menalled, L.B., 2005. Knock-in mouse models of Huntington's disease. NeuroRx. 2, 465–470.
Menalled, L.B., et al., 2002. Early motor dysfunction and striosomal distribution of huntingtin microaggregates in Huntington's disease knock-in mice. J. Neurosci. 22, 8266–8276.
Menalled, L.B., et al., 2003. Time course of early motor and neuropathological anomalies in a knock-in mouse model of Huntington's disease with 140 CAG repeats. J. Comp. Neurol. 465, 11–26.
Mihm, M.J., et al., 2007. Cardiac dysfunction in the R6/2 mouse model of Huntington's disease. Neurobiol. Dis. 25, 297–308.
Morton, A.J., et al., 2000. Progressive formation of inclusions in the striatum and hippocampus of mice transgenic for the human Huntington's disease mutation. J. Neurocytol. 29, 679–702.
Morton, A.J., et al., 2005. A combination drug therapy improves cognition and reverses gene expression changes in a mouse model of Huntington's disease. Eur. J. Neurosci. 21, 855–870.
Ordway, J.M., et al., 1997. Ectopically expressed CAG repeats cause intranuclear inclusions and a progressive late onset neurological phenotype in the mouse. Cell 91, 753–763.
Orr, H.T., Zoghbi, H.Y., 2007. Trinucleotide repeat disorders. Annu. Rev. Neurosci. 30, 575–621.
Pal, A., et al., 2008. Regulation of endosome dynamics by Rab5 and Huntingtin-HAP40 effector complex in physiological versus pathological conditions. Methods. Enzymol. 438, 239–257.
Penney Jr., J.B., et al., 1990. Huntington's disease in Venezuela: 7 years of follow-up on symptomatic and asymptomatic individuals. Mov. Disord. 5, 93–99.
Reddy, P.H., Williams, M., Charles, V., Garrett, L., Pike-Buchanan, L., Whetsell Jr, W.O., Tagle, D.A., 1998. Behavioral abnormalities and selective neuronal loss in HD transgenic mice expressing mutated full-length HD cDNA. Nat. Genet. 20, 198–202.
Ribchester, R.R., et al., 2004. Progressive abnormalities in skeletal muscle and neuromuscular junctions of transgenic mice expressing the Huntington's disease mutation. Eur. J. Neurosci. 20, 3092–3114.
Rosas, H.D., Hevelone, N.D., Zaleta, A.K., Greve, D.N., Salat, D.H., Fischl, B., 2005. Regional cortical thinning in preclinical Huntington disease and its relationship to cognition. Neurology 65, 745–747.
Rosas, H.D., et al., 2002. Regional and progressive thinning of the cortical ribbon in Huntington's disease. Neurology 58, 695–701.
Rosas, H.D., et al., 2008. Cerebral cortex and the clinical expression of Huntington's disease: complexity and heterogeneity. Brain 131, 1057–1068.
Rubinsztein, D.C., et al., 1996. Phenotypic characterization of individuals with 30–40 CAG repeats in the Huntington disease (HD) gene reveals HD cases with 36 repeats and apparently normal elderly individuals with 36–39 repeats. Am. J. Hum. Genet. 59, 16–22.
Schilling, G., Becher, M.W., Sharp, A.H., Jinnah, H.A., Duan, K., Kotzuk, J.A., Slunt, H.H., Ratovitski, T., Cooper, J.K., Jenkins, N.A., Copeland, N.G., Price, D.L., Ross, C.A., Borchelt, D.R., 1999. Intranuclear inclusions and neuritic aggregates in transgenic mice expressing a mutant N-terminal fragment of huntingtin. Hum. Mol. Genet. 8, 397–407.
Semaka, A., et al., 2006. Predictive testing for Huntington disease: interpretation and significance of intermediate alleles. Clin. Genet. 70, 283–294.
Seneca, S., et al., 2004. Early onset Huntington disease: a neuronal degeneration syndrome. Eur. J. Pediatr. 163, 717–721.
Sharp, A.H., et al., 1995. Widespread expression of Huntington's disease gene (IT15) protein product. Neuron. 14, 1065–1074.
Shelbourne, P.F., Killeen, N., Hevner, R.F., Johnston, H.M., Tecott, L., Lewandoski, M., Ennis, M., Ramirez, L., Li, Z., Iannicola, C., Littman, D.R., Myers, R.M., 1999. A Huntington's disease CAG expansion at the murine Hdh locus is unstable and associated with behavioral abnormalities in mice. Hum. Mol. Genet. 8, 763–774.
Slow, E.J., van Raamsdonk, J., Rogers, D., Coleman, S.H., Graham, R.K., Deng, Y., Oh, R., Bissada, N., Hossain, S.M., Yang, Y.Z., Li, X.J., Simpson, E.M., Gutekunst, C.A., Leavitt, B.R., Hayden, M.R., 2003. Selective striatal neuronal loss in a YAC128 mouse model of Huntington disease. Hum. Mol. Genet. 12, 1555–1567.
Solomon, A.C., et al., 2007. Verbal episodic memory declines prior to diagnosis in Huntington's disease. Neuropsychologia 45, 1767–1776.
Stack, E.C., et al., 2005. Chronology of behavioral symptoms and neuropathological sequela in R6/2 Huntington's disease transgenic mice. J. Comp. Neurol. 490, 354–370.
Stine, O.C., et al., 1993. Correlation between the onset age of Huntington's disease and length of the trinucleotide repeat in IT-15. Hum. Mol. Genet. 2, 1547–1549.
Strong, T.V., et al., 1993. Widespread expression of the human and rat Huntington's disease gene in brain and nonneural tissues. Nat. Genet. 5, 259–265.
Sun, Y., et al., 2001. Polyglutamine-expanded huntingtin promotes sensitization of *N*-methyl-D-aspartate receptors via post-synaptic density 95. J. Biol. Chem. 276, 24713–24718.
Tallaksen-Greene, S.J., et al., 2005. Neuronal intranuclear inclusions and neuropil aggregates in HdhCAG(150) knockin mice. Neuroscience. 131, 843–852.
Van Raamsdonk, J.M., et al., 2005a. Selective degeneration and nuclear localization of mutant huntingtin in the YAC128 mouse model of Huntington disease. Hum. Mol. Genet. 14, 3823–3835.
Van Raamsdonk, J.M., et al., 2005b. Cognitive dysfunction precedes neuropathology and motor abnormalities in the YAC128 mouse model of Huntington's disease. J. Neurosci. 25, 4169–4180.
von Horsten, S., et al., 2003. Transgenic rat model of Huntington's disease. Hum. Mol. Genet. 12, 617–624.
Vonsattel, J.P., et al., 1985. Neuropathological classification of Huntington's disease. J. Neuropathol. Exp. Neurol. 44, 559–577.
Warby, S., et al., 2008. Huntington disease. www.genetests.org.
Weeks, R.A., et al., 1996. Striatal D1 and D2 dopamine receptor loss in asymptomatic mutation carriers of Huntington's disease. Ann. Neurol. 40, 49–54.
Wheeler, V.C., et al., 2000. Long glutamine tracts cause nuclear localization of a novel form of huntingtin in medium spiny striatal neurons in HdhQ92 and HdhQ111 knock-in mice. Hum. Mol. Genet. 9, 503–513.
Wheeler, V.C., et al., 2002. Early phenotypes that presage late-onset neurodegenerative disease allow testing of modifiers in Hdh CAG knock-in mice. Hum. Mol. Genet. 11, 633–640.
Willner, P., 1991. Neuromethods. 18.
Woodman, B., et al., 2007. The Hdh(Q150/Q150) knock-in mouse model of HD and the R6/2 exon 1 model develop comparable and widespread molecular phenotypes. Brain Res. Bull. 72, 83–97.
Yu, Z.X., et al., 2003. Mutant huntingtin causes context-dependent neurodegeneration in mice with Huntington's disease. J. Neurosci. 23, 2193–2202.
Zuccato, C., et al., 2003. Huntingtin interacts with REST/NRSF to modulate the transcription of NRSE-controlled neuronal genes. Nat. Genet. 35, 76–83.